endocrines

MDPI

Article

Islet Amyloid Polypeptide Analogues with Reduced Aggregation: Implications for Type 2 Diabetes

Shahab Hassan [1], Sasha L. Evans [2], James H. Torpey [2], Tam Bui [3], Rivka L. Isaacson [2], Kenneth White [1] and Cassandra Terry [1,*]

[1] Centre for Health and Life Sciences Research, London Metropolitan University, Holloway Road, London N7 8DB, UK; shh0805@my.londonmet.ac.uk (S.H.); kenneth.white@londonmet.ac.uk (K.W.)
[2] Department of Chemistry, King's College London, London SE1 1DB, UK; sasha.1.evans@kcl.ac.uk (S.L.E.); james.h.torpey@gsk.com (J.H.T.); rivka.isaacson@kcl.ac.uk (R.L.I.)
[3] Biomolecular Spectroscopy Centre, Optical & Chiroptical Spectroscopy Facility, The Wolfson Wing, Hodgkin Building, King's College London, London SE1 1UL, UK; tam.bui@kcl.ac.uk
* Correspondence: c.terry@londonmet.ac.uk

Abstract

Background: Type 2 diabetes is projected to affect millions of people annually as the number of cases rises year on year. This includes children. Treating diabetes and its related comorbidities has a huge economic impact and puts pressure on healthcare providers. Understanding the disease at a molecular level is key for developing better therapeutics. The protein Islet Amyloid Polypeptide (IAPP) or amylin is important for glucose regulation; however, it is also instrumental in type 2 diabetes pathology. Human IAPP can misfold into oligomers and amyloid fibrillar aggregates within pancreatic islets, promoting β-cell dysfunction and death, contributing to progressive insulin deficiency and worsening hyperglycaemia. Methods: Based on previous studies on mutations at residues 18, 28 and 31,we have designed three novel IAPP analogues (two double and one triple mutant) to assess whether the combined amino acid substitutions impact fibril formation, solubility and toxicity. Results: All three of our analogues show a reduced propensity to aggregate and are more soluble than wild type IAPP. Compared with pramlintide, a clinically prescribed synthetic analogue of human amylin, all of our analogues appeared to have similarly reduced toxicity and improved solubility relative to human IAPP. Additionally, two of our analogues exhibited a markedly slower rate of fibril formation. Conclusions: Our results highlight the importance of targeting multiple residues as a promising strategy for developing improved diabetes therapeutics in the future.

Keywords: Islet Amyloid Polypeptide; hIAPP; amylin; type 2 diabetes mellitus; amyloid; analogues; therapeutics

Academic Editors: Daniela Foti and Eusebio Chiefari

Received: 2 March 2026
Revised: 18 May 2026
Accepted: 5 June 2026
Published: 9 June 2026

1. Introduction

Islet Amyloid Polypeptide (IAPP), commonly known as amylin, is a highly conserved protein co-expressed, co-processed, and co-secreted with insulin by the pancreatic islet cells to regulate blood glucose levels [1]. IAPP is a 37 amino acid protein containing a disulphide bond between Cys2 and Cys7 and is post-translationally modified by amidation at the C-terminal tyrosine. Described as an intrinsically disordered protein, it is soluble and monomeric in solution under physiological conditions. IAPP is composed of a N terminal domain (residues 1–19) that binds to membranes and insulin, an amyloidogenic core (20–29), and the C-terminal region (30–37) which is involved in self-association [2].

Analogues of human IAPP (hIAPP) have previously been researched as potential therapeutics for diabetes [3]. Pramlintide acetate (also known as Symlin) is an approved drug prescribed with insulin [4]. It is an amylin analogue that controls blood sugar by increasing satiety, reducing glucagon levels and influencing gastric emptying. It is similar in structure to IAPP; however, its amino acid sequence has been altered to resemble the rat sequence (rIAPP). Both rIAPP and pramlintide have proline residues at positions 25, 28, and 29, which replace the alanine and serine residues found in human IAPP, hIAPP (A25P, S28P, S29P). This region was investigated because residues within 20–29 are associated with amyloid formation, which is implicated in the pathogenesis of type 2 diabetes in humans [5]. The proline substitutions in rIAPP and pramlintide disrupt β-sheet formation and prevent fibril assembly [6].

The formation of amyloid fibrils is linked to over fifty different human diseases known as 'protein misfolding, 'protein aggregation' or 'amyloid' disorders such as Alzheimer's disease, Parkinson's disease, and type 2 diabetes [7,8]. Amyloid deposits of IAPP are found in pancreatic islets in the majority of those with type 2 diabetes and contribute to the progressive loss of pancreatic β-cells [9]. Living with type 2 diabetes has been linked to the onset of several fatal degenerative conditions such as Alzheimer's disease [10] highlighting the need to better understand and manage type 2 diabetes. Amyloidogenic proteins undergo conformational changes during aggregation, often involving a transition from α-helical to β-sheet-rich structures. This process typically proceeds from monomers to soluble oligomers, followed by protofibrils and eventually mature fibrils, which commonly consist of two or more protofilaments [11]. Mature amyloid fibrils are characterised by a cross-β sheet architecture, which can be detected using real-time assays such as thioflavin T fluorescence [11,12].

Whilst pramlintide works for many as a treatment for type 2 diabetes, it can cause unwanted side effects, has limited solubility and forms amyloid fibrils under certain conditions [13]. Pramlintide cannot be administered at physiological pH (pH 7.0–7.4) due to its instability so must be stored at pH 4.0 and cannot be co-administered with insulin. Whilst the structure of recombinant fibrils [14] and ex vivo fibrils isolated from patients with diabetes has been recently reported [5], understanding the impact of different amino acid residues on the function of IAPP, especially its solubility, toxicity and amyloid formation are still key to understanding its role in diabetes pathogenesis. Previous experiments have mutated individual residues of hIAPP to see their effect on fibril formation, solubility and toxicity [15]. H18R has been reported to reduce toxicity but is not able to prevent fibril formation [16]. S28P, found in rIAPP, is reported to abolish amyloid formation [17]. N31D was reported to slow amyloid formation and increase solubility [18]. Based on our earlier work [14], and literature analysis, strategic mutations were combined to produce analogue 1 (H18R S28P), analogue 2 (S28P N31D) and analogue 3 (H18R S28P N31D). Our study focused on elucidating the biophysical properties of these three analogues. These were systematically analysed for solubility, toxicity and propensity to form fibrils. The novelty of this study lies in the generation of multiple mutations and their comprehensive characterisation using a range of analytical techniques. Analogues were evaluated against several control samples (amyloid forming Hen Egg White Lysozyme and insulin, plus pramlintide) in the two commonly used buffers (Tris and PBS), enabling direct comparison with prior studies [14].

Our in vitro analyses show that all analogues showed a reduction in propensity to aggregate; compared to hIAPP and in comparison to pramlintide, two of our analogues demonstrated a markedly slower rate of fibril formation.

2. Materials and Methods

All procedures were carried out at room temperature and reagents were supplied by Sigma-Aldrich (SigmaAldrich.com) (Burlington, MA, USA) unless otherwise stated. Rat IAPP (rIAPP) was used as a negative control throughout whilst Hen Egg White Lysozyme (HEWL) and insulin were used as positive controls. Recombinant pramlintide and pramlintide acetate salt were used as a comparison for all experiments. All proteins were prepared to the same protein concentration in the same buffers as the analogues being tested, unless otherwise stated.

2.1. Analogue Design

All analogues were designed to have increased isoelectric point, solubility, and a reduced propensity to aggregate and form amyloid fibrils compared to hIAPP. Isoelectric point and solubility were assessed using ProtParam [19] available on the ExPASy server (https://web.expasy.org/protparam/) accessed on 10 September 2024 and Aggrescan4D software (https://biocomp.chem.uw.edu.pl/a4d/) accessed on 10 September 2024 respectively using the mutated amino acid sequence as input. The propensity to aggregate and form amyloid fibrils was assessed using Aggrescan4D. NMR structures of human (PDB ID: 2L86) and rat IAPP (PDB ID: 2KJ7) were used as inputs for human (hIAPP, pramlintide and analogues) or for rIAPP, respectively. In all cases, Chain A was selected for analysis and the distance for aggregation analysis was set at 10 Å. The following settings were enabled: pH-dependent calculations, stability calculations and disabled, analysis of globular regions, dynamic mode, improve protein solubility with evolutionarily conserved mutations, enhance protein solubility with charged mutations. For hIAPP and rIAPP sequences, static mode was used to assess aggregation based on the native structure. For analogues 1–3, mutate mode was employed using PDB code 2L86 as template.

2.2. Preparation of Peptide Stock Solutions

Three peptide analogues were produced by mutating the key residues H18R, S28P and N31D: analogue 1 (H18R S28P) analogue 2 (S28P N31D) and analogue 3 (H18R S28P N31D). Analogues, produced by GenScript (GenScript.com), incorporated a C-terminal amidated tyrosine and a disulphide bridge between residues 2–7. Analogues were purified by Liquid Chromatography–Mass Spectrometry to >95% purity and tested for solubility in 0.1M PBS, pH 7.4, DMSO and 8M Urea. Freeze-dried peptides were dissolved in 100% hexafluoro isopropanol (HFIP) at 21 °C to a final concentration of 1.6 mM and incubated for 2 h without agitation. The peptide solutions were snap-frozen in liquid nitrogen for 5 min and subsequently lyophilized for 24 h. Lyophilized peptides were stored at −80 °C until further use. Prior to use, peptides were reconstituted in either 10 mM phosphate-buffered saline (PBS, 10 mM phosphate-buffered saline containing 137 mM NaCl, 2.7mM KCl) or 20 mM Tris-HCl buffer (both at pH 7.4). Protein concentrations were determined using a Pierce BCA Protein Assay Kit (Thermo Scientific, Waltham, MA, USA).

2.3. SDS-PAGE

Proteins were separated using an 18% polyacrylamide resolving gel (0.375 M Tris-HCl, 0.1% SDS, pH 8.8) and 4% stacking gel (0.125 M Tris-HCl, 0.1% SDS, pH 6.8). Gels were prepared using ProtoGel 40% acrylamide/bis-acrylamide solution (37.5:1, catalogue no. EC-891), 4× ProtoGel resolving buffer (1.5 M Tris-HCl, 0.4% SDS, pH 8.8, catalogue no. EC-892), and 4× ProtoGel stacking buffer (0.5 M Tris-HCl, 0.4% SDS, pH 6.8, catalogue no. EC-893). Ammonium persulfate and TEMED were added to a final concentration of 0.1% (*w*/*v*) for polymerization. SeeBlue™ Plus2 Pre-stained Protein Standard were used as molecular weight markers. Protein samples were prepared using 4X protein loading

buffer (LI-COR Biosciences, Lincoln, NE, USA) supplemented with 2-mercaptoethanol to a final concentration of 10% (*w*/*v*). Samples were denatured at 95 °C for 5 min and briefly centrifuged before loading. Gels were run at 110 V for 90 min, stained with Coomassie Brilliant Blue R-250 (0.25% *w*/*v* Coomassie R-250, 10% acetic acid, 40% methanol) and destained using 10% acetic acid, 20% methanol. Gels were imaged using LI-COR Odyssey CLx imaging system.

2.4. Solubility Measurements

Lyophilised peptides and control samples were dissolved in either 10 mM PBS or 20 mM Tris-HCl buffer (pH 7.4) at 16 μM concentration. Solutions were incubated at 25 °C for 7 days without agitation. After incubation, samples were centrifuged at 1.6×10^4 *g* for 20 min using a Biofuge Pico (Heraeus) microfuge, Fisher Scientific, Loughborough, UK. The absorbance of the supernatant was measured at 280 nm using a FLUOstar Omega microplate reader (BMG Labtech, Aylesbury, UK) to estimate relative peptide solubility. All peptide analogues contained the same number of tyrosine, phenylalanine, and disulfide bonds, and lacked tryptophan residues, ensuring identical extinction coefficients. Experiments were repeated in triplicate (technical replicates) and mean values and error bars showing standard deviation plotted.

2.5. Optimised Thioflavin T (ThT) Assay

Assays were set up using protein samples at 16 μM concentration and Thioflavin T at 32 μM concentration in 20 mM Tris-HCl or 10 mM PBS at pH 7.4. Reactions were set up in 96 well black plates (Cat. No. 655075, Greiner Bio-One, Stonehouse, UK) in triplicate at 25 °C to a final volume of 100 μL and repeated at least three times. Mean values and error bars showing standard deviations were plotted to show the variability of the readings. HEWL was used as our fibril control. 1 mM HEWL was dissolved in 0.5M glycine buffer, 70 mM NaCl, pH 2.0 and incubated with 50 μM ThT at 37 °C with constant agitation at 250 RPM for 12 days. Fluorescence was measured using a FLUOstar Omega plate reader (S/N 415-0735) with excitation and emission wavelengths of 448 nm and 482 nm, respectively. Measurements were taken over 24 h with plates briefly shaken (5 s) prior to readings being taken.

2.6. Transmission Electron Microscopy (TEM)

Samples were set up in parallel to thioflavin T experiments and freshly prepared for loading onto grids. After 18 h, 3 μL sample aliquots were applied to 300 mesh carbon-coated copper grids (Agar Scientific, Rotherham, UK) and incubated for 2 min. Excess sample was blotted with filter paper then grids stained with 3% (*w*/*v*) uranyl acetate for 30 s, followed by blotting to remove excess stain. Grids were allowed to fully air-dry before storing until needed. All images were acquired using a JEOL JEM-1400 transmission electron microscope (JEOL UK Ltd, Watchmead, UK). Multiple grids of separate technical repeats (3) were analysed. Typically, 50 grid squares were analysed per grid and representative images of the grid shown.

2.7. Circular Dichroism

Lyophilised peptide stock solutions were prepared to 25 μM concentration in either 20 mM Tris-HCl or 10 mM PBS buffer (containing 140 mM KCl, no NaCl) pH 7.4, in Eppendorf tubes with gentle agitation at 25 °C for 18 h. Far-UV measurements were taken using an Applied Photophysics Chirascan™-Plus spectrometer (Leatherhead, Surrey, UK). Absorbance and CD readings were taken at a target temperature of 23 °C, controlled using a Quantum Northwest TC 125 Temperature Control. Near-UV and far-UV CD readings were taken at 400–230 nm, 2 nm Bandwidth (BW), 1 nm SS (Step Size), 1 s Time per Point (TpP) and 260–190 nm, 2 nm BW, 1 nm SS, 1.36 s TpP respectively. Ten millimetre (near-UV CD region)

and 0.5 mm (far-UV CD region) rectangular cuvettes were employed. Air in the chamber and buffer control were auto subtracted as the background from all readings. A Savitzky–Golay filter was applied to smooth the CD reading at 190–260 nm. Collected data was then processed using the Applied Photophysics Pro-Data Chirascan application (version 4.5). The far-UV CD spectra were normalised for concentration, pathlength and expressed in terms of De ($M^{-1}cm^{-1}$).

2.8. MTT Cell Viability Assay

To assess whether IAPP analogues are cytotoxic to cells, cell viability of INS-1 cells (rat insulinoma cell line) was measured following treatment with analogues. Cells were seeded at a density of 5000 cells per well in a flat-bottom, clear 96-well tissue culture plate (Corning, New York, NY, USA). Cells with passage number <30 were maintained in RPMI-1640 medium with L-Glutamine (Cat. No. L0500-500; Biowest, Nuaille, France) supplemented with 10% (v/v) fetal bovine serum (FBS) and 1% (v/v) penicillin–streptomycin (Cat. No. 15140122; Gibco™, Loughborough, UK). After plating, cells were allowed to adhere and stabilise by incubating the plate for 24 h at 37 °C in a humidified atmosphere containing 5% CO_2. Following incubation, analogues were freshly prepared to a final concentration of 16 µM concentration from 10 x stock solutions in either 10 mm PBS or 20 mM Tris HCl at pH 7.4 by adding stock peptides in a 1:10 ratio to RPMI-1640 complete culture. A total of 100 µL of each freshly prepared analogue was loaded onto each well and exposed to treatment for 24 h.

After 24 h, 100 µL of MTT (3-[4,5-dimethylthiazol-2-yl]-2,5 diphenyl tetrazolium bromide, Cat. No. 158990010, Thermo Scientific Chemicals, Waltham, MA, USA) working solution (0.5 mg/mL in culture medium) was added to each well, and the plate incubated for 3 h at 37 °C to allow metabolically active cells to reduce MTT to formazan crystals. The medium was carefully removed, and 100 µL of DMSO added to each well to solubilise the formazan crystals. Absorbance was measured at 570 nm using a FLUOstar Omega microplate reader (BMG Labtech, Ortenberg, Germany). Cell viability was calculated as a percentage relative to untreated control wells. All experiments were performed in at least triplicate and independently repeated three times. The data is presented as mean values ± standard deviation from three independent biological experiments combined, each with three replicates.

3. Results

3.1. Rationally Designed Analogues

Double and triple mutant analogues of hIAPP (analogue 1 H18R S28P, analogue 2 S28P N31D, analogue 3 H18R S28P N31D) were designed to incorporate substituted residues 18, 28, 31 and combining them allowed us to evaluate their additive effects. A sequence comparison can be seen in Figure 1 with changed residues (18, 28 and 31) highlighted in red showing how they differ from hIAPP. In parallel, for all experiments, our analogues were compared to rIAPP, hIAPP and recombinant pramlintide and pramlintide acetate. RIAPP is reported to not form fibrils [6] and hence act as our negative control. It has been well established that hIAPP does [2]. Pramlintide, the only analogue available and approved for authorisation used in the United States, is reported to not form fibrils since it is based on the rIAPP sequence [4]. Both rIAPP and pramlintide have proline residues at positions 25, 28, and 29 yet their sequence differs at residue at residues 18, 23 and 26. Pramlintide has H18 (like hIAPP) Phe23, and Ile26, while rIAPP has Arg18, Leu23, and Val26. We also attempted to produce another double mutant H18R N31D; however, despite multiple attempts, were unsuccessful. The presence of substantial changes in charges at positions 18 and 31 of the peptide, without concomitant alterations or stabilisation at

position 28, may account for the fragmentation found when utilising a conventional peptide synthesis methods. The successful synthesis of triple mutant (H18R S28P N31D) supports this theory.

Figure 1. Sequence comparison of analogues, rIAPP, hIAPP and pramlintide. Each peptide contains a C-terminal amidated tyrosine and a disulphide bond between C2 and C7. Residues highlighted in red indicate amino acid changes that differ from hIAPP.

Aggrescan4D was used to assess the potential impact of mutating residues 18, 28 and 31 on the structure of hIAPP, and comparing them to rIAPP and pramlintide (Figure 2). Aggrescan4D was selected over AlphaFold 3 (https://alphafoldserver.com/welcome) because the experimental structure of the base sequence (hIAPP) used to generate the analogues was already known (PDB ID: 2L86). This enables a direct and reliable comparison of residue-specific aggregation propensities using the physicochemical and knowledge-based scoring approach implemented in Aggrescan4D. All structures have a conserved N-terminal loop stabilised by disulphide bonds (Cys2-Cys7) and a short helix plus a flexible unstructured C-terminus. Our analogues are predicted to structurally resemble pramlintide (Figure 2B) rather than rIAPP (Figure 2A) featuring an 'L-shaped' or 'helix-kink-helix' structure that is a transient intermediate structure required for binding to cell membranes [2]. Changes in predicted structure can be observed especially in the C-terminal region where residues 28 and 31 have been mutated (Figure 2D–F).

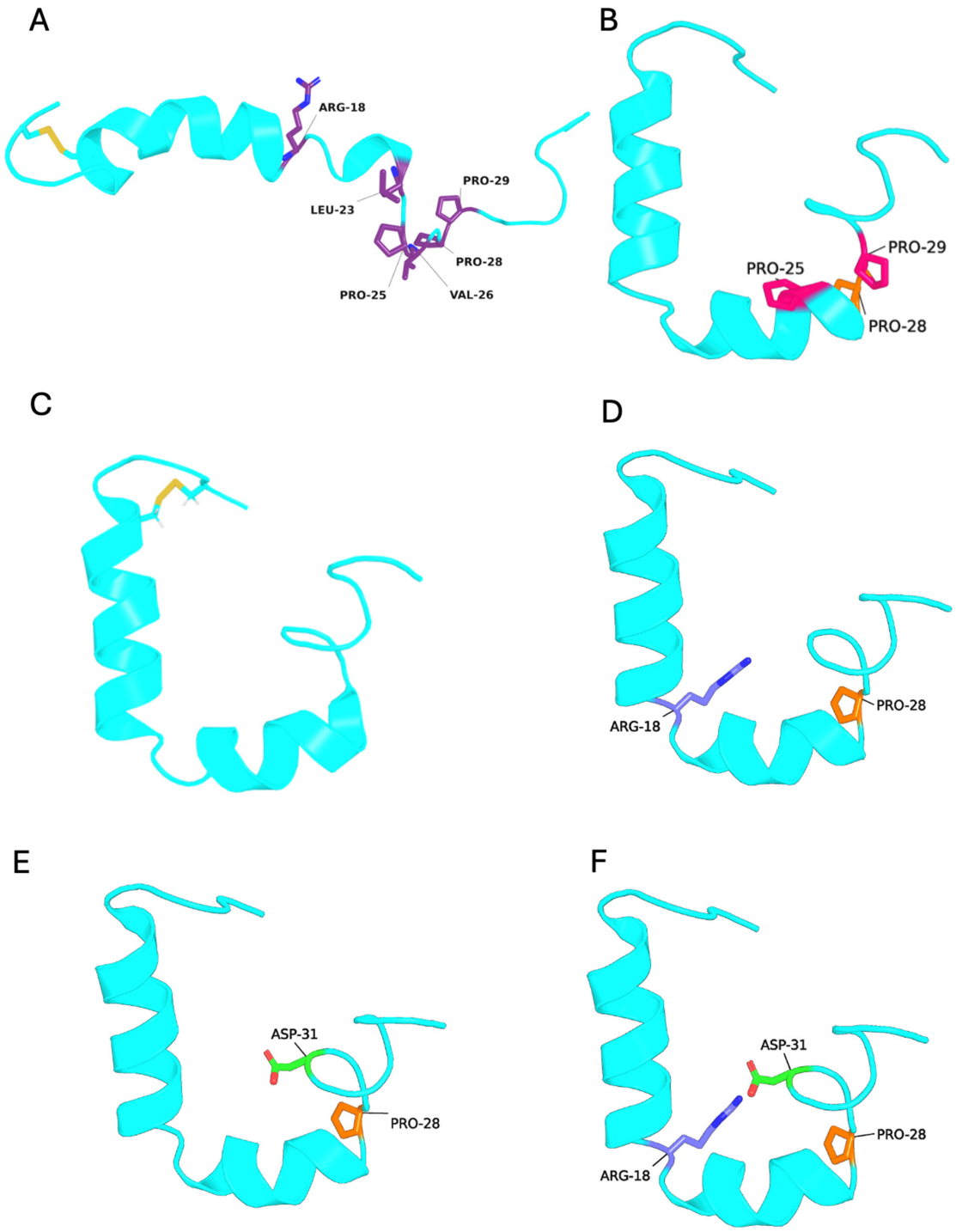

Figure 2. Structural representation of analogues, rIAPP, hIAPP and pramlintide. The structure of analogues were predicted using Aggrescan4D with key substituted residues shown. (**A**) rIAPP, (**B**) pramlintide, (**C**) hIAPP, (**D**) analogue 1 (H18R S28P), (**E**) analogue 2 (S28P N31D), and (**F**) analogue 3 (H18R S28P N31D). Residues in rIAPP that differ from hIAPP are highlighted in purple in (**A**). Proline substitutions in Pramlintide that differ from the human sequence are shown in pink and orange. Substituted residues in the analogues are shown in blue (residue 18), orange (residue 28) and green (residue 31) in (**D**–**F**), also highlighted in the pramlintide structure (**B**). Disulfide bonds are highlighted in yellow. Each peptide is shown N-terminus to C-terminus from left to right. Structures in panels (**A**,**B**) were rendered from PDB entries 2KJ7 and 2L86, respectively. Structures in panels (**C**–**F**) were predicted using Aggrescan4D. All structures were rendered using PyMOL version 3.1.0.

3.2. Prediction of Solubility and Aggregation Propensity

All analogues were designed with isoelectric points (calculated using ProtParam) compatible with solubility at physiological pH 7.4 (Table S1). The predicted instability index values (<40) indicated that all analogues were stable at pH 7.4 whilst aliphatic index values indicative of thermostability, suggested all proteins were stable between 20 and 45 °C. Grand average of hydropathicity (GRAVY) values (−0.472 and −0.01) suggested good solubility and hydrophilicity of all analogues under these conditions.

All designed analogues were predicted to have a lower aggregation propensity than hIAPP and pramlintide, and higher than rIAPP (Tables S2 and S3). We used Aggrescan4D to predict aggregation-prone regions based on hydrophobicity, β-structure propensity, and dynamic structural factors to provide per-residue aggregation scores and a global score for each sequence, before confirming in vitro. HIAPP exhibits the highest total score and average score indicating a strong overall aggregation propensity, consistent with previous experimental observations [17] being similar to pramlintide. rIAPP, in contrast, shows a negative total (−0.35) and average score (−0.0094), reflecting a significantly lower tendency to aggregate, in agreement with its known resistance to fibril formation [2,6]. Our novel analogues show intermediate aggregation profiles, with total scores between 8.30 and 9.43. These results suggest that all three analogues retain some aggregation propensity relative to rIAPP but are likely to be less amyloidogenic than hIAPP and pramlintide.

The residue-specific profiles (Table S3) reveal the impact of residues 18, 28 and 31 on aggregation. Residue 18, (located near the N-terminal edge of the amyloidogenic core, residues 20–29) shows hIAPP and pramlintide to have a near-neutral score (0.05 and 0.09), whilst rIAPP and analogues 1–3 have negative values (−0.41 to −0.75), suggesting reduced local aggregation propensity at this site. Residue 28 consistently exhibits strong positive scores (≈1.0–1.2) across all peptides, linking this region to aggregation. This aligns with its location within the amyloidogenic core (residues 20–29) of IAPP. Residue 31, located C-terminal to the core region, shows strongly negative scores in analogues 1–3 reflecting local suppression of aggregation in this region. These values contrast to pramlintide which has a predicted positive value (1.2) at this residue.

3.3. Analogue Characterisation and Solubility

Purity and mass of all analogues were first confirmed by SDS-PAGE (Figure 3) revealing that all analogues had a mass of 3.9 kDa and were pure. The poor solubility of hIAPP can be observed under these conditions (Figure 3, lane 5). The solubility of each analogue was then tested in 10 mM PBS buffer and 10 mM Tris (pH 7.4), the two most utilised buffers by other researchers. The aim was to assess whether changing specific amino acids greatly improved the solubility of hIAPP, reported as being poor at physiological pH [20]. Ideally this would have been measured at a physiological temperature; however, issues with evaporation at 37 °C led to reactions being undertaken at 25 °C.

After being incubated for 7 days at 25 °C (without agitation), solubility was compared with hIAPP, with all samples at 16 μM concentration, conditions used previously by other researchers [14]. The apparent solubility of the samples was approximated by the absorbance of the supernatant at 280 nm. Overall, proteins proved less soluble (or even insoluble) in PBS compared to Tris (Figure 4). Only analogue 1 (H18R S28P), analogue 2 (28P N31D) and recombinant pramlintide showed any solubility in PBS. In Tris, the positive controls (HEWL and insulin) showed relatively good solubility. Analogue 2 (S28P N31D) and 3 (H18R S28P N31D) were more soluble than hIAPP with comparable solubility to pramlintide, yet both were more soluble in PBS than all the other samples. Analogue 1 (H18R S28P) is comparable in solubility to hIAPP. rIAPP and pramlintide were less soluble than hIAPP.

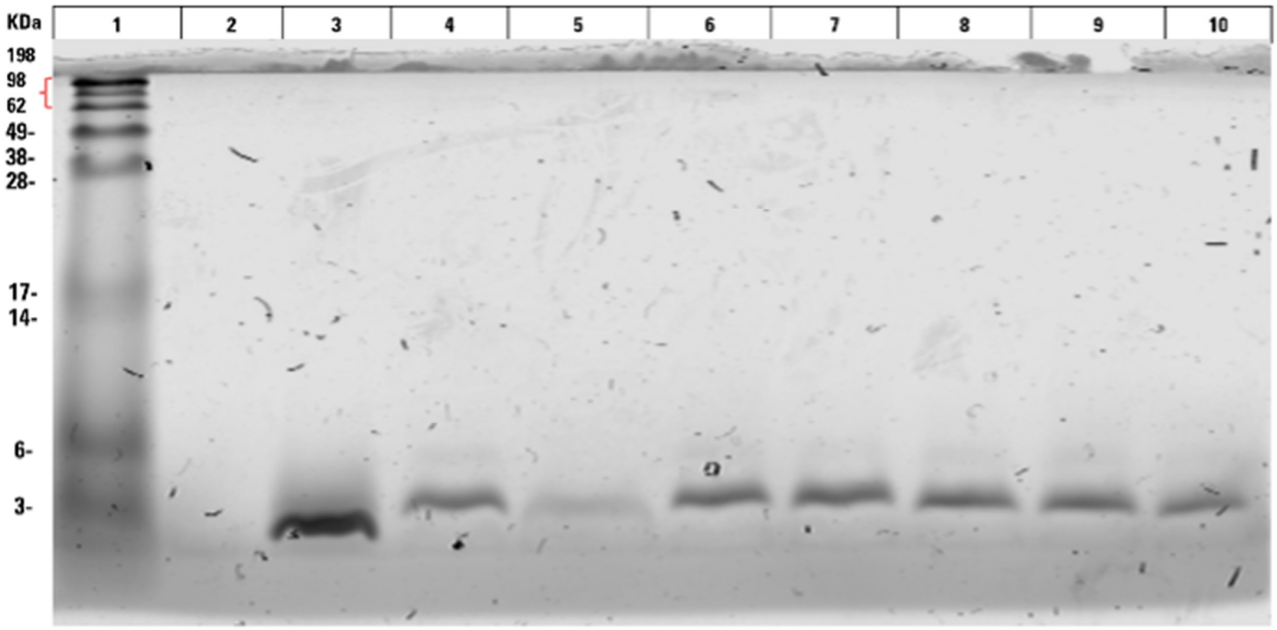

Figure 3. SDS-PAGE analysis of samples stained with Coomassie Brilliant Blue confirming analogue purity and mass. Proteins were separated using an 18% SDS-PAGE gel with a 4% stacking gel. Lane 1 contains SeeBlue™ Plus2 Pre-stained Protein Standards. Lane 2 is PBS buffer only. Lane 3–10 contain 7.5 µg of the following proteins: insulin, rIAPP, hIAPP, analogue 1(H18R S28), analogue 2 (S28P N31D) analogue 3 (H18R S28P N31D), pramlintide acetate and recombinant pramlintide respectively. Experiments were repeated several times (technical replicates) and a representative gel is shown.

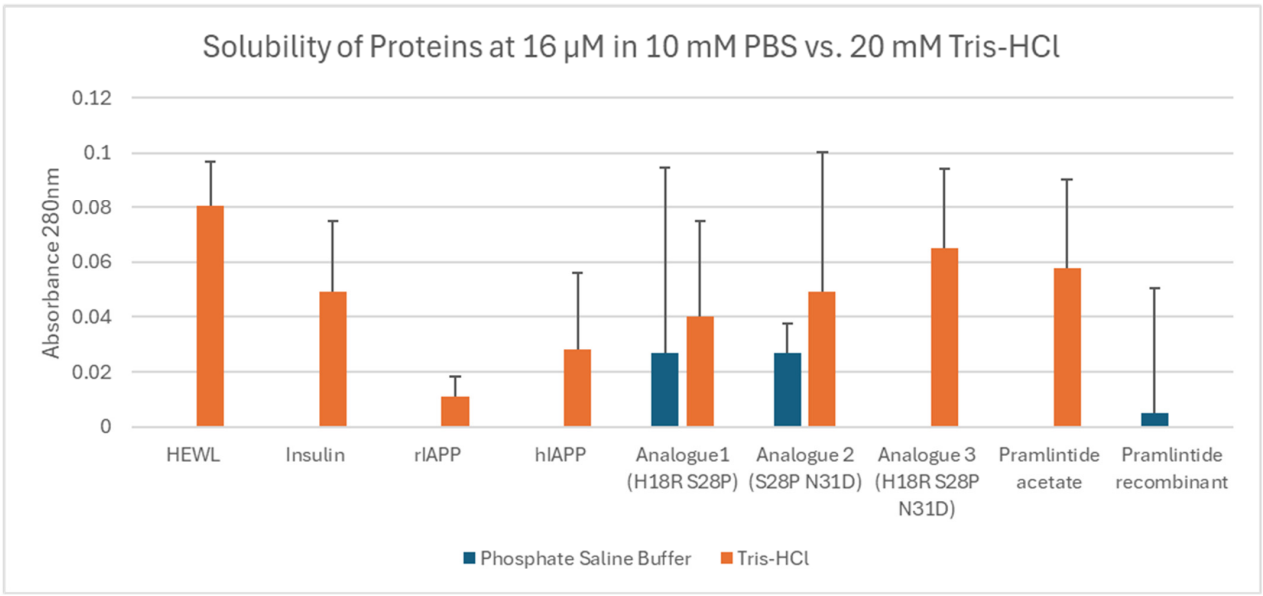

Figure 4. Increased solubility of protein samples in Tris compared to PBS when incubated at a concentration of at 16 µM for 7 days at 25 °C without agitation. The amount of protein remaining in the supernatant after centrifugation represents the soluble fraction reflected in the absorbance at 280 nm. Mean values of 3 technical repeat experiments and standard deviations are shown (error bars).

3.4. Measuring Amyloid Formation

Since hIAPP can readily form amyloid fibrils under certain conditions, we investigated whether the combined amino acid substitutions introduced in our analogues abolish or slow the rate of amyloid formation. Thioflavin T assays were used to detect fibril formation in real-time. Pre-formed HEWL fibrils acted as a positive control (Figure S1A).

Analogues were monitored over a period of 24 h in both Tris and PBS buffers, conditions similar to previous studies [14]. Thioflavin T aggregation kinetics were calculated to quantitatively compare the different samples (Table 1). Where possible, half-time (t½) values were determined from the midpoint of the fitted sigmoidal curves, but in some cases sigmoidal curves were not produced (Figure 5) making kinetic analysis difficult (e.g., hIAPP). HIAPP exhibited the most rapid aggregation followed by insulin, analogue 3, recombinant pramlintide, pramlintide acetate, analogue 1, analogue 2 then rIAPP (which did not form fibrils). Excluding rIAPP, analogue 2 had the slowest lag time taking 17 h to start forming fibrils. All analogues had lower F_{Max} values (plateau) than insulin, pramlintides and hIAPP.

Table 1. Thioflavin T kinetics. The lag time (T_{lag}) is defined as the time interval before the rapid, exponential increase in ThT fluorescence. The half time ($T_{½}$) represents the time required for the ThT fluorescence intensity to reach half of its maximum amplitude (plateau). The maximum fluorescence (F_{Max}) is the average maximum amplitude (plateau) reached. * denotes that aggregation occurred too rapidly to reliably determine t ½ under the experimental conditions. $ denotes that the plateau phase was not reached after 24 h; however, values were determined from 48 h reactions.

Sample	Lag Time T_{lag} (Hours)	Half Time $T_{½}$ (Hours)	Maximum Fluorescence F_{Max} (AU)
Insulin	0.0	1.33	3250
rIAPP	N/A	N/A	0
hIAPP	0.0	*	4000
Analogue 1 (H18R S28P)	18.0	24.00	600 $
Analogue 2 (S28P N31D)	17.00	25.00	1500 $
Analogue 3 (H18R S28P N31D)	4.00	7.00	4500
Pramlintide acetate	6.00	9.33	1900
Recombinant pramlintide	8.00	9.17	1600

In Tris, hIAPP formed fibrils most readily, followed by insulin (Figure 5), plateauing at 2 and 5 h respectively. The negative control sample rIAPP did not form fibrils, as expected [6]. Recombinant pramlintide and pramlintide acetate did form fibrils but at a significantly reduced rate compared to hIAPP, plateauing at 10 h. Analogues 1 (H18R S28P) and 2 (S28P N31D) had a markedly reduced fibril formation rates, with lag times of 17/18 h before fibrils started to form. In comparison to hIAPP, analogue 3 (H18R S28P N31D) formed fibrils more slowly (starting after 4 h) with a steep exponential phase plateauing between 10 and 22 h after which no further increase in Thioflavin signal was observed.

Results in PBS were considerably different. HIAPP readily formed fibrils almost instantaneously whereas none of the other samples did (Figure S2).

These results correlate with the structural predictions in Figure 2. Aggrescan 4D predictions show that our analogues adopt a pramlintide-like "L-shaped" helix–kink–helix amphipathic structure, which favours a compact, kinked conformation rather than an extended β-sheet formation. The proline-induced kink stabilises this non-linear, membrane-interacting helix and prevents the transition into the extended β-sheet geometry required for amyloid fibril nucleation and growth, thereby reducing fibril formation.

To confirm Thioflavin T assay observations, negative-stain TEM was used to determine the aggregation state of all samples, noting the presence or absence of structures, mainly fibrils. Samples were set up in parallel and freshly loaded onto grids after incubating at 25 °C for 18 h. As expected from thioflavin T observations, in PBS and Tris, HEWL readily formed twisted fibrils (Figure 6A and Figure S1) up to 250 nm in length and <10 nm wide. Insulin, another protein

known to readily form fibrils [21], formed fibrils up to 500 nm in length and 10–15 nm wide, in Tris buffer only (Figure 6B). There were also oligomers visible in the sample circular, up to 25 nm wide, indicative of pre-fibrillar material. HIAPP, formed fibrils in Tris and PBS buffer (Figure 6C and Figure S2). They measured <500 nm in length and ~15 nm wide, composed of two twisted protofilaments. Some visible oligomers (up to 20 nm) could also be seen alongside fibrils, again suggesting the presence of pre-fibrillar material. Analogue 3 (H18R S28P N31D) contained some fibrillar material ~15 nm in width (Figure 6D); however, they were not abundant which was surprising since thioflavin T experiments suggested that it could readily form fibrils (Figure 5). Fibrils were visible in both pramlintide samples (Figure 6E,F) measuring up to 15 nm wide confirming thioflavin T observations.

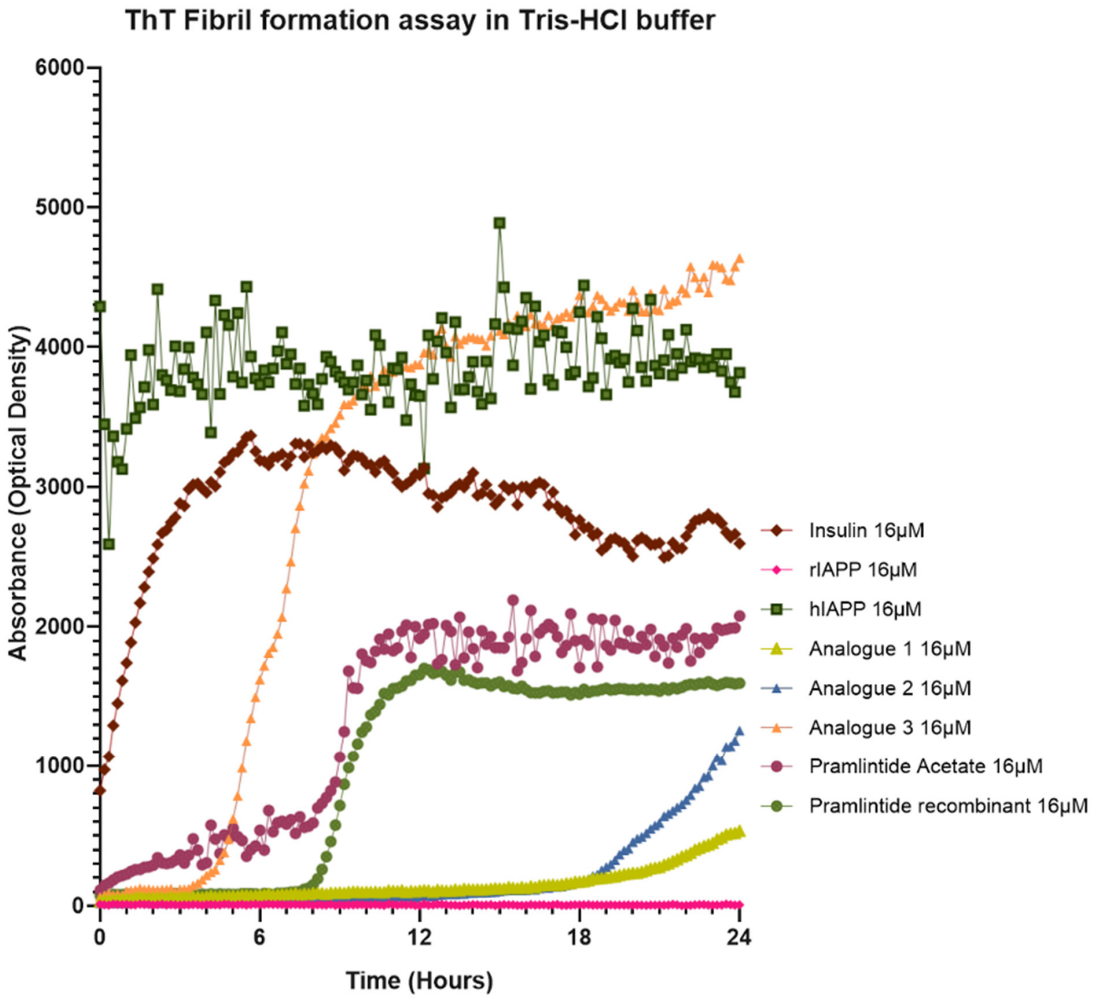

Figure 5. Thioflavin T assays revealed that all analogues had a longer lag phase compared to hIAPP, taking longer to form fibrils. Assays were performed using 16 μM protein and 32 μM thioflavin T in 20 mM Tris-HCl (pH 7.4). Experiments were performed in triplicate. Fluorescence readings were recorded every 10 min and data presented as the mean fluorescence intensity of triplicate samples. Data are representative of several technical repeat experiments.

No other structures were observed for any of the other samples analysed (rIAPP, analogue 1, analogue 2), consistent with thioflavin T observations, after extensive analysis with multiple samples. Many of the samples were challenging to image since fibrils tended to clump together in huge aggregates which may explain the limited fibrils observed for analogue 3. It is important to note that TEM images are representative and may not reflect overall sample heterogeneity.

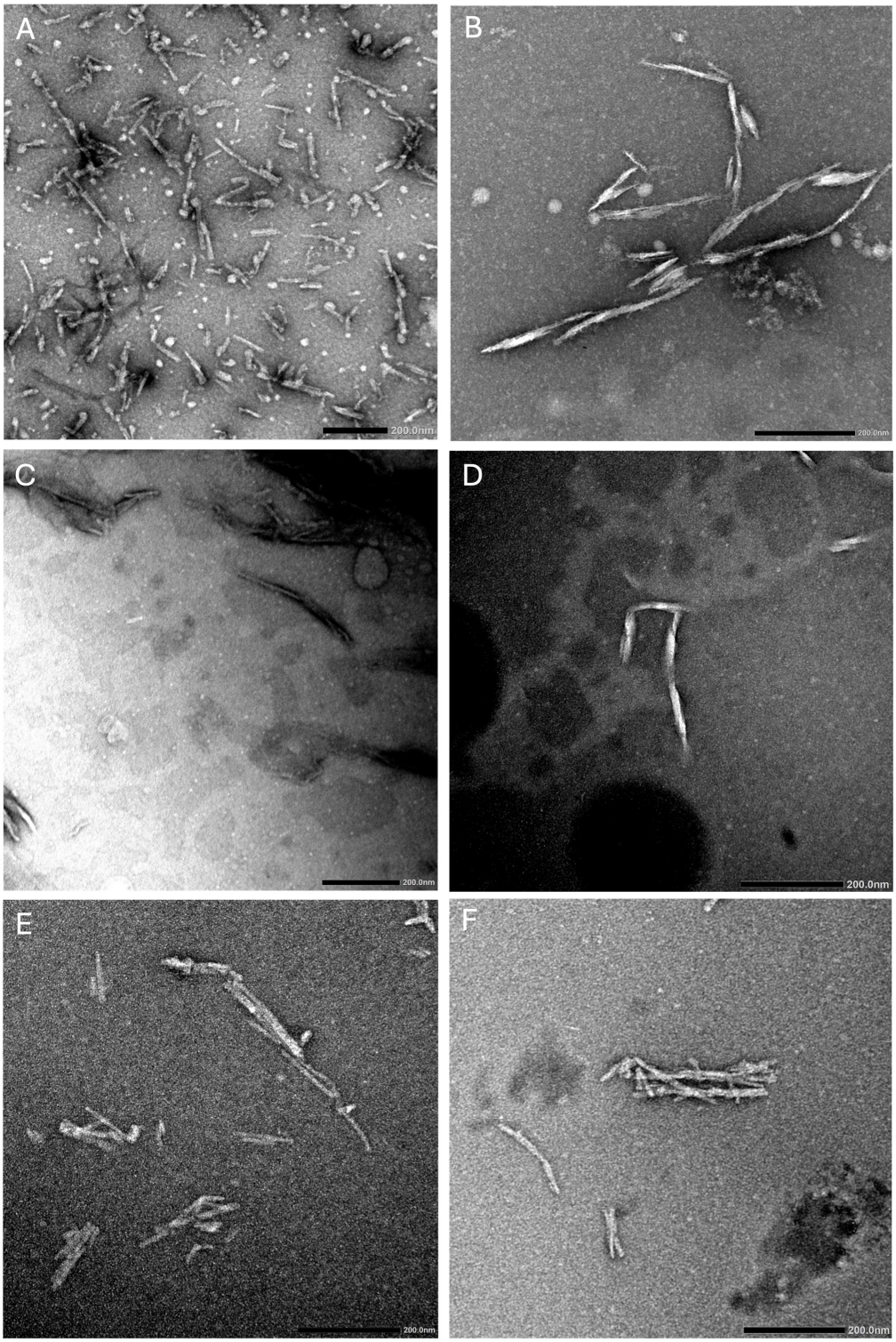

Figure 6. TEM micrographs showing samples that contained fibrils. (**A**) HEWL (**B**) insulin (**C**) hIAPP (**D**) analogue 3 (H18R S28P N31D) (**E**) pramlintide acetate and (**F**) recombinant pramlintide formed fibrils in thioflavin T assays after 18 h using 20 mM Tris. Images are representative of observations obtained from three independent technical replicates for each sample. Scale bars 200 nm.

3.5. Analysis of Secondary Structure Using Circular Dichroism

In parallel to Thioflavin T experiments, we analysed our samples by circular dichroism to ascertain what secondary structure elements were present. We wanted to confirm that fibrils were present in the samples that contained high fluorescence readings. Samples incubated for 18 h in either Tris or PBS were measured to see whether they contain

β-sheet structures indicative of amyloid fibril formation. Protein concentrations had to be increased for both Tris and PBS samples, increasing from 16 μM concentration used previously to 25 μM concentration. In Tris buffer, positive peaks observed for HEWL and insulin at 190–195 nm and a negative peak 205–210 nm was indicative of β-sheets (Figure 7). However, some α-helices may also be present since negative peaks at 208 nm are also evident. HIAPP gave almost no signal. For all other samples, no characteristic features consistent with β-sheet conformations were observed. Negative peaks ~200 nm are indicative of random coil/irregular secondary structure. In PBS, no significant peaks were observed for any of the samples except for rIAPP that had a broad negative peak at 200–205 nm indicative of random coil/disordered protein structure (Figure S2C).

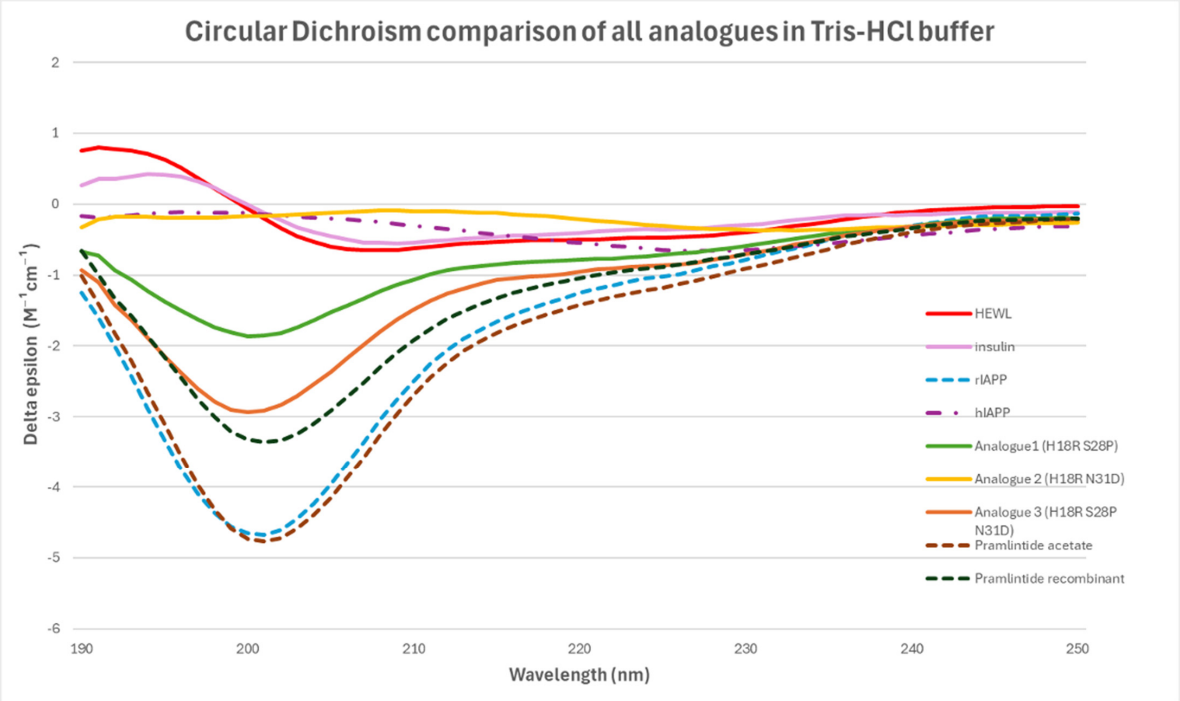

Figure 7. Circular dichroism analysis of samples to investigate their secondary structure content. Positive and negative peaks at 190–195 and 205–210 shown for HEWL and insulin are indicative of β-sheet content. Negative peaks at 200 nm observed for all other samples, are indicative of random coil. Samples containing α -helical content are indicated by negative peaks ~208 and 222 nm.

This was likely due to poor sample solubility in PBS at increased protein concentrations (25 μM) and the interference of chloride ions with signals below 200 nm (Figure S2). Since CD requires high protein concentrations and peptide availability was limited, lower concentrations were used, likely contributing to the weak signals observed in both buffers and the absence of a detectable β-sheet signal in samples containing fibrils by TEM. Since our samples were not centrifuged or separated prior to analysis, samples likely contained mixed populations (monomers, oligomers, amyloid fibrils) as observed by TEM (Figure S2B).

3.6. Assessing Cell Toxicity

To assess whether our analogues are toxic to mammalian cells, for preliminary screening we tested their effects on a rat insulinoma mammalian cell line (INS-1 cells). Cell viability was tested using an MTT assay. The same concentration used for the previous biochemical analyses (16 μM) was added to cells for 24 h in either Tris (Figure 8A) or PBS (Figure 8B). Similar trends were observed using both buffers. Our assays suggested that all analogues were less toxic to cells than hIAPP, demonstrated by higher percentage viability values. Analogue 2 (S28P N31D) exhibited the lowest toxicity, comparable to pramlintide

and rIAPP. HEWL fibrils (100 μM concentration) and 10% DMSO served as positive controls inducing the lowest cell viability and thus highest toxicity to cells.

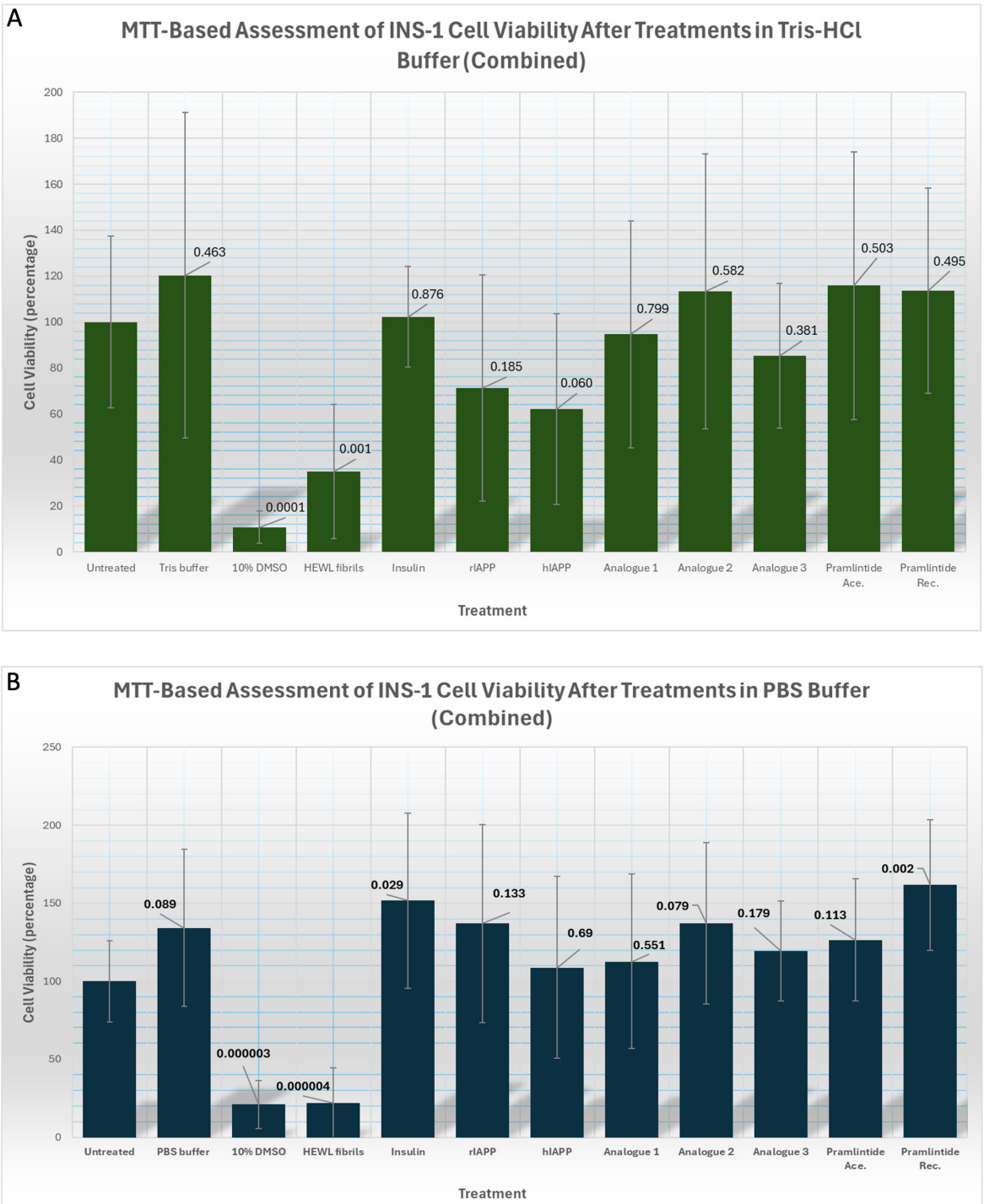

Figure 8. MTT cell viability assays were used to measure cell toxicity and showed that all analogues were less toxic to cells than hIAPP and comparable to pramlintide. Cell viability was assessed after 24 h incubation with samples. INS-1 cells were treated with protein samples at 16 μM concentration prepared in (**A**) 20 mM Tris or (**B**) 10 mM PBS, pH 7.4. Controls included untreated cells, PBS buffer in media, 10% DMSO and 100 μM HEWL fibrils (used at 100 μM). The data shows mean ± SD combined of three independent biological replicates, each performed in triplicate. *p*-value were calculated by comparing untreated group against each treatment group. Differences in cell viability were analysed using an unpaired, two-tailed student *t*-test with unequal variance (Welch's *t*-test) using a significance level of $\alpha = 0.05$. *p*-values above 0.05 do not show a significant increase in cell viability.

The aim of our work was to produce analogues that had improved biophysical properties superior to pramlintide in terms of solubility, toxicity and reduced aggregation. We have collated our results to summarise how our analogues compare to pramlintide in Table 2. We have specifically focused on pramlintide acetate rather than recombinant pramlintide since pramlintide acetate is the synthetic analogue used as a therapeutic for diabetes [4]. Compared to pramlintide acetate (t½ = 9 h 20 min), analogues 1 (t½ = 24 h) and 2 (t½ = 25 h) had reduced rates of aggregation, since t ½ is the time required for the fluorescence signal to reach 50% of its maximum value (F_{max}). Both have increased lag times (18 h and 17 h) compared to pramlintide (6 h) taking much longer to form fibrils and reduced F_{max} rates reaching a much lower fluorescence read out. In contrast, analogue 3 (t½ = 7 h) forms fibrils more readily compared to pramlintide with a shorter lag time, shorter t½ and a higher F_{max}. Analogues 1 and 2 are more soluble in PBS. Our toxicity assays suggest that analogue 2 is less toxic to cells in PBS but shows comparable toxicity to pramlintide in Tris. However, these results have only been tested in a single cell line and further validation is required.

Table 2. Comparing the biochemical and biophysical properties of analogues 1–3 with pramlintide acetate shows that analogue 2 has improved properties. All samples were compared to data observed in Figures 4–6 and 8. For comparison, pramlintide acetate has calculated T_{lag}, $T_{1/2}$ and F_{max} of 6.0, 9.3 and 1900 respectively.

Sample	More Soluble?	Aggregation Kinetics	TEM Observations	Less Toxic?
Analogue 1 (H18R S28P)	No (Tris) Yes (PBS)	T_{lag} = 18 h $T_{1/2}$ = 24 h F_{max} 600 AU	No fibrils (Tris or PBS)	No (Tris) No (PBS)
Analogue 2 (S28P N31D)	Comparable (Tris) Yes (PBS)	T_{lag} = 17 h $T_{1/2}$ = 25 h F_{max} 1500 AU	No fibrils (Tris or PBS)	Comparable (Tris) Comparable (PBS)
Analogue 3 (H18R S28P N31D)	Comparable (Tris) No (PBS)	T_{lag} = −4 h $T_{1/2}$ = 7 h F_{max} = 4500 AU	Fibrils (Tris) No fibrils (PBS)	No (Tris) No (PBS)

4. Discussion

4.1. Biophysical and Biochemical Findings

Given the association between aggregated forms of hIAPP and type 2 diabetes [1,14], this study aimed to investigate the biochemical and biophysical properties of hIAPP through targeted mutations at key residues, through assessing their combined impact on solubility, cytotoxicity, and aggregation propensity. The strategy of this study focussed on combining mutated residues and conducting all our experiments in both Tris and PBS buffers so we could compare them to previous studies [22,23]. We also included several control samples [21,24] plus rIAPP, hIAPP and pramlintide to provide a comprehensive analysis. Analogues were also analysed using several biochemical and biophysical techniques to consolidate findings. For example, the results of our Thioflavin T assays were confirmed by TEM and CD as false-positive fluorescence signals (due to non-specific binding of Thioflavin T) as has been previously reported [25,26].

Our analogues were designed to be more structurally similar to pramlintide than rIAPP (Figure 2) in order to maintain human compatibility and preserve receptor activity, initially focusing on residues 20–29, a region critical for amyloid formation [3]. The S28P substitution, observed in rIAPP, is known to abolish amyloid formation [17] so this mutation was incorporated in all of our analogues. Proline substitutions are well-established β-sheet breakers.

Due to the absence of an amide hydrogen, proline cannot participate in the backbone hydrogen bonding required for β-sheets and thus prevents β-sheet stabilisation [17,27,28]. This disrupts β-sheet stacking and inhibits amyloid fibril formation [17,27,28] consistent with reduced aggregation observed for our analogues 1 (H18R S28P) and 2 (S28P N31D). As expected, rIAPP did not form fibrils under these conditions whereas hIAPP did (Figure S2) as previously observed [20]. There was no TEM or CD evidence to indicate that analogue 1 (H18R S28P) or analogue 2 (S28P N31D) formed amyloid fibrils (Figures 6, 7 and S2). Analogue 3 (H18R S28P N31D) formed fibrils at a reduced rate compared to hIAPP in Tris buffer (Figures 5 and 6) but not in PBS (Figure S2).

The impact of our combined mutations on aggregation kinetics can be observed in Figure 5 and Table 1. The long lag time of 18 h, half time of 24 h and maximum fluorescence of 600 AU for analogue 1 may be explained by H18R and S28P synergistically suppressing both the kinetics of nucleation and the structural propagation of β-sheet-rich fibrils, shifting toward soluble or nonfibrillar states rather than mature amyloid assemblies although TEM observations did not reveal any structures. H18R introduces a permanently charged arginine at residue 18, increasing electrostatic repulsion and peptide solvation [29] which reduces formation of aggregation-competent conformations and destabilises early oligomeric nuclei. S28P directly disrupts the amyloidogenic core region (residues 20–29) by introducing proline, a strong β-sheet breaker [17,27,28]. This can impair steric zipper formation, inhibit nucleus assembly, destabilise protofibril elongation, and reduce secondary nucleation on fibril surfaces.

For analogue 2, S28P and N31D may suppress both early nucleation and later fibril propagation, favouring soluble or off-pathway nonfibrillar aggregates rather than mature amyloid fibrils. Whilst no structures were observed by TEM, our Thioflavin T assays reflect this showing a long lag time of 17 h and a half time of 25 h. N31D replaces asparagine with negatively charged aspartate near the fibril core, introducing electrostatic repulsion and reducing favourable side-chain hydrogen-bonding interactions that normally stabilise cross-β packing and fibril maturation [30]. Since residue 31 participates in intermolecular contacts within assembled fibrils, the mutation may also destabilise protofibrils and lower secondary nucleation efficiency.

For analogue 3, in theory, H18R S28P N31D should target multiple mechanistic stages of the fibrillation pathway simultaneously, including monomer misfolding, primary nucleation, β-sheet propagation, and fibril maturation [17,18,29], as we predicted when designing our analogues with a reduced propensity to aggregate (Tables S2 and S3). However, analogue 3 is still able to readily form fibrils (Figures 5 and 6) albeit with a longer lag time (4 h) and half time (7 h) than hIAPP (Table 1). Although H18R increases electrostatic repulsion, S28P disrupts β-sheet continuity, and N31D destabilises intermolecular packing [17,29,30], the peptide still retains much of the highly amyloidogenic hydrophobic core sequence (especially F23–L27), allowing monomers to associate and form early nuclei relatively efficiently. Since nucleation can still occur through residual hydrophobic collapse and partial β-structure formation [31], the lag phase is only modestly extended. The mutations may also raise the energetic barrier for facilitating primary nucleation but not entirely abolish the early association of monomers. Primary nucleation is driven by multiple transient hydrophobic and backbone-mediated contacts across the peptide, especially within residues 20–29 so even with S28P disrupting local β-sheet geometry and H18R and N31D introducing electrostatic penalties, partially ordered oligomeric assemblies may still form through residual hydrophobic interactions, e.g., F23, A25, I26, and L27 [31]. Future experimental exploration is warranted to further test our hypotheses.

Importantly, all three analogues appeared less toxic to INS-1 cells compared to hIAPP (Figure 8). Changing residue 18 (H18R), found in rIAPP, resulted in analogues 1 (H18R S28P) and analogue 3 (H18R S28P N31D) appearing less toxic to INS-1 cells than hIAPP as previously

observed [16]. This could be due to arginine increasing the net charge of the protein and local charge at residue 18, preventing H18R hIAPP from embedding and damaging cell membranes [29]. Analogue 2 which did not contain H18R, also appeared less toxic to cells than hIAPP. This could be attributed to the combined effect of proline at residue 28 and aspartate at reside 31 disrupting formation of β-sheet rich oligomers that can contribute to toxicity [20]. N31D has been reported to destabilise the C-terminal region, critical for cross-β amyloid formation, thereby diminishing the propensity to form fibrils or oligomers that can induce β-cell toxicity by creating holes in the membranes [18,30].

All three analogues showed better solubility than rIAPP and hIAPP when using Tris buffer (Figure 4). Substituting asparagine with aspartic acid at residue 31 (analogues 2 and 3), results in better solubility as previously reported [18] since aspartic acid is highly hydrophilic and thus enhances solubility through electrostatic repulsion.

Our observations fit with our hypothesis and align with previous studies incorporating single substitutions. In comparison to hIAPP, analogue 1 (H18R S28P) has reduced toxicity [16] and reduced amyloid formation [17]. Analogue 2 (S28P N31D) has reduced amyloid formation [17] and increased solubility [18]. Analogue 3 (H18R S28P N31D) has reduced toxicity [16], slower rate of fibril formation [17] and increased solubility [18]. Further experiments are needed to determine the precise molecular mechanisms.

4.2. Study Design and Future Challenges

Our results demonstrate that buffer composition is a critical experimental variable not only for IAPP but also for other amyloid-forming proteins such as insulin [21], as parallel experiments conducted in Tris and PBS yielded markedly different results. These findings emphasise the importance of using standardised conditions to ensure reproducible and interpretable results in studies of amyloidogenic proteins, particularly when they are being evaluated in vitro in an exploratory context as potential therapeutic candidates.

Previous studies have analysed IAPP samples in HFIP; however, this does not mimic physiological conditions and is toxic to mammalian cells even at low concentrations [32], hence why we avoided this. Analysing samples at physiological temperature (37 °C) was attempted; however, this was not feasible due to the rapid rate of fibril formation and increased evaporation. Therefore, we selected 25 °C, consistent with previous studies [33].

Whilst our observations relied largely on fibrillar assemblies, we cannot discount the influence that the presence of oligomers or pre-fibrillar assemblies may have on our findings. The presence of oligomers was only observed by TEM for certain samples; however, it is likely that all of our samples contained species of multiple aggregation states. Due to their transient nature, it is difficult to study intermediate species; however, oligomers have been shown to be associated with β-cell toxicity [34]. Future studies with our analogues should investigate ways to separate them for further analysis using techniques such as dynamic light scattering or size exclusion chromatography. This will determine how distinct morphologies correlate with observed biochemical and biophysical results and how they relate to pathology.

Whilst predictive software informed the rational design of our analogues, some discrepancies between its predictions (Tables S1–S3) and our experimental observations highlight the critical importance of laboratory validation, especially with analogue 3.

Whilst our analogues, especially analogue 2 showed promise in terms of reduced amyloid formation, toxicity and increased solubility compared to hIAPP and pramlintide (Table 2), our findings are limited to in vitro analysis so future experiments need to include in vivo testing. This will account for important in vivo factors such as post translational modifications, protein–protein interactions, crowding effects and the influence of the lipid environment [30,35]. Utilising membrane-mimicking systems (liposomes) in future work

will assess the influence of lipids on IAPP aggregation. Since in vitro and ex vivo IAPP fibrils differ in structure [5] as observed in other amyloid disorders [36,37] the need for in vivo analysis of IAPP is further recommended.

4.3. Implications for Type 2 Diabetes

As cases of type 2 diabetes rise every year [14], molecular level understanding is key to improving therapeutics.

Metformin remains the most popular therapeutic for type 2 diabetes management due to its cost effectiveness. However, Metformin cannot be prescribed to those with renal impairment, liver disease, heart failure or those at risk of lactic acidosis limiting its use [14]; hence, alternative treatments such as amylin analogues are needed.

We tested pramlintide in parallel to our analogues so we could see how they compare in terms of biophysical properties (Table 2). Limited solubility and the propensity to form fibrils limit pramlintide's use as a therapeutic [13]. This was reflected in some of our observations. Analogues 1 and 2 took much longer to form fibrils compared to Pramlintide ($T_{1/2}$ of 24 and 25 h compared to 9 h) and much lower F_{max} values (600, 1500, compared to 1900) as shown in Figure 5 and Table 1. Additionally Pramlintide acetate was completely insoluble in PBS after 7 days at 25 °C yet analogues 1 and 2 showed some soluble material (Figure 4). Another limitation of pramlintide is that it cannot be administered at physiological pH due to its instability so must be stored at pH 4.0 and cannot be co-administered with insulin. Our analogues are predicted to be structurally stable under physiological conditions (Table S1); however, experimental evaluation of their stability is still needed and will be explored in future studies.

A better understanding of the physiological role of IAPP in glucose regulation is key for preserving the beneficial metabolic effects whilst minimising the formation of pathological forms during rational peptide design. Since our analogues form fibrils more slowly than hIAPP in vitro, our results relate to this key pathological process in type 2 diabetes where misfolding and aggregation of IAPP leads to amyloid fibril deposition in pancreatic islets, which is strongly associated with β-cell stress, β-cell apoptosis and progressive loss of insulin secretion and worsening hyperglycaemia [9].

Our results suggest that targeting multiple residues may represent a promising exploratory strategy for the potential development of improved diabetes therapeutics in the future. Mutating single residues has limited effect in promoting favourable drug-like properties [6]; however, mutating two residues resulted in analogues 1 (H18R S28P) and 2 (S28P N31D) possessing markedly slower fibril formation rates and comparable apparent toxicity and solubility to Pramlintide (Table 2). These results link peptide design and protein aggregation with core endocrine questions, namely how IAPP contributes to β-cell dysfunction in type 2 diabetes and how aggregation-resistant analogues might be developed for therapeutic use. At present, however, our results are restricted to in vitro experiments, are purely exploratory and have not been tested for therapeutic efficacy.

4.4. Future Considerations

Whilst our observations are exploratory at this stage, future strategies could focus on developing analogues similar to the amylin agonists Cagrilintide, Petrelintide and Eloralintide. These provide benefits including extended half-lives, better receptor signalling, enhanced stability and reduced daily administrations respectively [15,38,39]. Importantly, any new analogue will need to be assessed in combination with insulin, as co-administration is the current strategy. Amylin receptor activation studies (such as cAMP accumulation assays), in vivo metabolic validation (such as LDH release assay or

caspase-3/7 activation assays), pharmacokinetics and analogue stability will also need to be investigated to assess their functional and biological relevance.

Recent Cryo-TEM experiments revealed that individual mutations (A25P, S28P, and S29P) that do not abolish fibril formation can result in the formation of fibrils distinct from hIAPP [6]. Understanding how specific residues are associated with fibril formation is key for understanding type 2 diabetes pathology. In addition, elucidating the structure and function of oligomers and pre-fibrillar IAPP intermediates warrants further study since they have been associated with β-cell death in patients with type 1 and type 2 diabetes [40].

Supplementary Materials: The following supporting information can be downloaded at https://www.mdpi.com/article/10.3390/endocrines7020028/s1, Table S1: Using ProtParam to calculate physical and chemical parameters of proteins based on its sequence; Table S2: Aggrescan4D was used to calculate aggregation propensity scores for our designed analogues; Table S3: Calculating aggregation propensity for residues 18, 28 and 31; Figure S1: Thioflavin T assays and TEM analysis of HEWL; Figure S2: Analysis of fibril formation in PBS buffer using Thioflavin T assays, TEM and CD analysis.

Author Contributions: Conceptualisation, C.T. and S.H.; methodology, C.T. and S.H.; software, S.H. and C.T.; validation, C.T., K.W. and S.H.; formal analysis, S.H., C.T. and K.W.; investigation, S.H., S.L.E., J.H.T.; resources, T.B., R.L.I.; data curation, C.T.; original draft preparation, C.T. and S.H.; reviewing and editing, all authors; visualisation, C.T. and S.H.; supervision, C.T. and K.W.; project administration, C.T.; funding acquisition, C.T., J.H.T., S.L.E., R.L.I. and T.B. All authors have read and agreed to the published version of the manuscript.

Funding: This research was partly funded by London Metropolitan University. TEM experiments were conducted at the Centre for Ultrastructural Imaging of King's College London and funded by grants from the Biotechnology and Biological Sciences Research Council (BBSRC) (BB/S006877/1 (J.H.T.), and BB/X001415/1 (S.L.E.) to R.L.I.). CD experiments were conducted at The KCL Centre for Biomolecular Spectroscopy and funded by the Wellcome Trust and the British Heart Foundation (Ref. 202767/Z/16/Z and IG/16/2/32273).

Institutional Review Board Statement: Not applicable.

Informed Consent Statement: Not applicable.

Data Availability Statement: The original contributions presented in this study are included in the article. Further inquiries can be directed to the corresponding author.

Acknowledgments: The authors gratefully acknowledge the Centre for Ultrastructural Imaging of King's College London for their support and expertise in carrying out this work. The authors are grateful to Elizabeth Sawyer (University of Westminster) for introducing us to Rivka Isaacson, who facilitated this collaboration enabling TEM analysis.

Conflicts of Interest: The authors declare no conflicts of interest. The funders had no role in the design of the study; in the collection, analyses, or interpretation of data; in the writing of the manuscript; or in the decision to publish the results.

Abbreviations

The following abbreviations are used in this manuscript:

IAPP	Islet Amyloid Polypeptide
TEM	Transmission Electron Microscopy
CD	Circular Dichroism
Cys	Cysteine
HEWL	Hen Egg White Lysozyme
MTT	3-[4,5-dimethylthiazol-2-yl]-2,5 diphenyl tetrazolium bromide

References

1. Sevcuka, A.; White, K.; Terry, C. Factors That Contribute to hIAPP Amyloidosis in Type 2 Diabetes Mellitus. *Life* **2022**, *12*, 583. [CrossRef] [PubMed] [PubMed Central]
2. Westermark, P.; Engström, U.; Johnson, K.H.; Westermark, G.T.; Betsholtz, C. Islet amyloid polypeptide: Pinpointing amino acid residues linked to amyloid fibril formation. *Proc. Natl. Acad. Sci. USA* **1990**, *87*, 5036–5040. [PubMed] [PubMed Central]
3. Adeghate, E.; Kalász, H. Amylin Analogues in the Treatment of Diabetes Mellitus: Medicinal Chemistry and Structural Basis of its Function. *Open Med. Chem. J.* **2011**, *5*, 78–81. [CrossRef] [PubMed] [PubMed Central]
4. Ryan, G.; Briscoe, T.A.; Jobe, L. Review of pramlintide as adjunctive therapy in treatment of type 1 and type 2 diabetes. *Drug Des. Dev. Ther.* **2009**, *2*, 203–214. [CrossRef] [PubMed] [PubMed Central]
5. Liu, W.; Han, J.; Gong, W.; Zhang, F.; Cao, Q. Structure of pancreatic hIAPP fibrils derived from patients with type 2 diabetes. *Cell* **2026**, *189*, 1201–1210.e10. [CrossRef] [PubMed]
6. Ooi, S.A.; Valli, D.; Kuska, M.I.; Marí, H.; Chaudhary, H.; Wahlgren, W.Y.; Westenhoff, S.; Tietze, A.A.; Novials, A.; Servitja, J.-M.; et al. Cryo-EM exposes diverse polymorphism in IAPP mutants to guide the rational design of peptide-based therapeutics. *J. Mol. Biol.* **2025**, *437*, 169405. [CrossRef] [PubMed]
7. Dobson, C.M.; Knowles, T.P.J.; Vendruscolo, M. The Amyloid Phenomenon and Its Significance in Biology and Medicine. *Cold Spring Harb. Perspect. Biol.* **2020**, *12*, a033878. [CrossRef] [PubMed] [PubMed Central]
8. Shome, G.; Mondal, R.; Deb, S.; Roy, J.; Mandal, A.K.; Benito-León, J. Bridging Pancreatic Amyloidosis and Neurodegeneration: The Emerging Role of Amylin in Diabetic Dementia. *Int. J. Mol. Sci.* **2025**, *26*, 5021. [CrossRef]
9. Cooper, G.J.; Willis, A.C.; Clark, A.; Turner, R.C.; Sim, R.B.; Reid, K.B. Purification and characterization of a peptide from amyloid-rich pancreases of type 2 diabetic patients. *Proc. Natl. Acad. Sci. USA* **1987**, *84*, 8628–8632. [CrossRef] [PubMed] [PubMed Central]
10. Szablewski, L. Associations Between Diabetes Mellitus and Neurodegenerative Diseases. *Int. J. Mol. Sci.* **2025**, *26*, 542. [CrossRef]
11. Kuzu, O.F.; Granerud, L.J.T.; Saatcioglu, F. Navigating the landscape of protein folding and proteostasis: From molecular chaperones to therapeutic innovations. *Signal Transduct. Target. Ther.* **2025**, *10*, 358. [CrossRef]
12. Naiki, H.; Higuchi, K.; Hosokawa, M.; Takeda, T. Fluorometric determination of amyloid fibrils in vitro using the fluorescent dye, thioflavin T1. *Anal. Biochem.* **1989**, *177*, 244–249. [CrossRef] [PubMed]
13. Lee, N.J.; Norris, S.L.; Thakurta, S. Efficacy and Harms of the Hypoglycemic Agent Pramlintide in Diabetes Mellitus. *Ann. Fam. Med.* **2010**, *8*, 542–549. [CrossRef] [PubMed] [PubMed Central]
14. Hassan, S.; White, K.; Terry, C. Linking hIAPP misfolding and aggregation with type 2 diabetes mellitus: A structural perspective. *Biosci. Rep.* **2022**, *42*, BSR20211297. [CrossRef] [PubMed]
15. Fischer Munch, H.; Just, R.; Mosolff Mathiesen, J.; Eriksson, P.O.; Skodborg Villadsen, J.; Vestergaard, B.; Deryabina, M.; Demmer, O.; Skarbaliene, J.; Hamprecht, D.W.; et al. Development of Petrelintide: A Potent, Stable, Long-Acting Human Amylin Analogue. *J. Med. Chem.* **2025**, *68*, 23925–23940. [CrossRef] [PubMed]
16. Khemtemourian, L.; Guillemain, G.; Foufelle, F.; Killian, J.A. Residue specific effects of human islet polypeptide amyloid on self-assembly and on cell toxicity. *Biochimie* **2017**, *142*, 22–30. [CrossRef]
17. Ridgway, Z.; Eldrid, C.; Zhyvoloup, A.; Ben-Younis, A.; Noh, D.; Thalassinos, K.; Raleigh, D.P. Analysis of Proline Substitutions Reveals the Plasticity and Sequence Sensitivity of Human IAPP Amyloidogenicity and Toxicity. *Biochemistry* **2020**, *59*, 742–754. [CrossRef] [PubMed] [PubMed Central]
18. Nguyen, P.T.; Zottig, X.; Sebastiao, M.; Bourgault, S. Role of Site-Specific Asparagine Deamidation in Islet Amyloid Polypeptide Amyloidogenesis: Key Contributions of Residues 14 and 21. *Biochemistry* **2017**, *56*, 3808–3817. [CrossRef]
19. Gasteiger, E.; Hoogland, C.; Gattiker, A.; Duvaud, S.; Wilkins, M.R.; Appel, R.D.; Bairoch, A. Protein Identification and Analysis Tools on the ExPASy Server. In *The Proteomics Protocols Handbook [Internet]*; Walker, J.M., Ed.; Humana Press: Totowa, NJ, USA, 2005; pp. 571–607. [CrossRef]
20. Wang, H.; Abedini, A.; Ruzsicska, B.; Raleigh, D.P. Rationally Designed, Nontoxic, Nonamyloidogenic Analogues of Human Islet Amyloid Polypeptide with Improved Solubility. *Biochemistry* **2014**, *53*, 5876–5884. [CrossRef] [PubMed] [PubMed Central]
21. Jiménez, J.L.; Nettleton, E.J.; Bouchard, M.; Robinson, C.V.; Dobson, C.M.; Saibil, H.R. The protofilament structure of insulin amyloid fibrils. *Proc. Natl. Acad. Sci. USA* **2002**, *99*, 9196–9201. [CrossRef] [PubMed] [PubMed Central]
22. Miller, M.E.T.; Li, M.H.; Baghai, A.; Peetz, V.H.; Zhyvoloup, A.; Raleigh, D.P. Analysis of Sheep and Goat IAPP Provides Insight into IAPP Amyloidogenicity and Cytotoxicity. *Biochemistry* **2022**, *61*, 2531–2545. [CrossRef]
23. Akter, R.; Bower, R.L.; Abedini, A.; Schmidt, A.M.; Hay, D.L.; Raleigh, D.P. Amyloidogenicity, Cytotoxicity, and Receptor Activity of Bovine Amylin: Implications for Xenobiotic Transplantation and the Design of Nontoxic Amylin Variants. *ACS Chem. Biol.* **2018**, *13*, 2747–2757. [CrossRef] [PubMed]
24. Brudar, S.; Hribar-Lee, B. The Role of Buffers in Wild-Type HEWL Amyloid Fibril Formation Mechanism. *Biomolecules* **2019**, *9*, 65. [CrossRef] [PubMed] [PubMed Central]

25. Hudson, S.A.; Ecroyd, H.; Kee, T.W.; Carver, J.A. The thioflavin T fluorescence assay for amyloid fibril detection can be biased by the presence of exogenous compounds. *FEBS J.* **2009**, *276*, 5960–5972. [CrossRef] [PubMed]
26. Noormägi, A.; Primar, K.; Tõugu, V.; Palumaa, P. Interference of low-molecular substances with the thioflavin-T fluorescence assay of amyloid fibrils. *J. Pept. Sci. Off. Publ. Eur. Pept. Soc.* **2012**, *18*, 59–64. [CrossRef] [PubMed]
27. Abedini, A.; Raleigh, D.P. Destabilization of human IAPP amyloid fibrils by proline mutations outside of the putative amyloidogenic domain: Is there a critical amyloidogenic domain in human IAPP? *J. Mol. Biol.* **2006**, *355*, 274–281. [CrossRef] [PubMed]
28. Chiu, C.-C.; Singh, S.; de Pablo, J.J. Effect of Proline Mutations on the Monomer Conformations of Amylin. *Biophys. J.* **2013**, *105*, 1227–1235. [CrossRef] [PubMed] [PubMed Central]
29. Brender, J.R.; Hartman, K.; Reid, K.R.; Kennedy, R.T.; Ramamoorthy, A. A Single Mutation in the Non-Amyloidogenic Region of IAPP (Amylin) Greatly Reduces Toxicity. *Biochemistry* **2008**, *47*, 12680–12688. [CrossRef] [PubMed] [PubMed Central]
30. Kiriyama, Y.; Nochi, H. Role and Cytotoxicity of Amylin and Protection of Pancreatic Islet β-Cells from Amylin Cytotoxicity. *Cells* **2018**, *7*, 95. [CrossRef]
31. Ziaunys, M.; Mikalauskaite, K.; Sakalauskas, A.; Smirnovas, V. Study of Insulin Aggregation and Fibril Structure under Different Environmental Conditions. *Int. J. Mol. Sci.* **2024**, *25*, 9406. [CrossRef]
32. Shimizu, T.; Nogami, E.; Ito, Y.; Morikawa, K.; Nagane, M.; Yamashita, T.; Ogawa, T.; Kametani, F.; Yagi, H.; Hachiya, N. Volatile Anesthetic Sevoflurane Precursor 1,1,1,3,3,3-Hexafluoro-2-Propanol (HFIP) Exerts an Anti-Prion Activity in Prion-Infected Culture Cells. *Neurochem. Res.* **2021**, *46*, 2056–2065. [CrossRef] [PubMed] [PubMed Central]
33. Wang, H.; Raleigh, D.P. The Ability of Insulin To Inhibit the Formation of Amyloid by Pro-Islet Amyloid Polypeptide Processing Intermediates Is Significantly Reduced in the Presence of Sulfated Glycosaminoglycans. *Biochemistry* **2014**, *53*, 2605–2614. [CrossRef] [PubMed]
34. Shivani, S.T.; LeMasters, B.E.; Ravula, T.; Esterly, H.J.; Maroli, N.; Rich, K.L.; Fields, C.R.; Dicke, S.S.; Warmuth, O.A.; Stapleton, D.S.; et al. A structural model of toxic amyloid oligomers involved in type 2 diabetes. *Proc. Natl. Acad. Sci. USA* **2026**, *123*, e2528103123. [CrossRef] [PubMed] [PubMed Central]
35. Höppener, J.W.M.; Jacobs, H.M.; Wierup, N.; Sotthewes, G.; Sprong, M.; de Vos, P.; Berger, R.; Sundler, F.; Ahrén, B. Human Islet Amyloid Polypeptide Transgenic Mice: In Vivo and Ex Vivo Models for the Role of hIAPP in Type 2 Diabetes Mellitus. *J. Diabetes Res.* **2008**, *2008*, 697035. [CrossRef]
36. Terry, C.; Wenborn, A.; Gros, N.; Sells, J.; Joiner, S.; Hosszu, L.L.P.; Tattum, M.H.; Panico, S.; Clare, D.K.; Collinge, J.; et al. Ex vivo mammalian prions are formed of paired double helical prion protein fibrils. *Open Biol.* **2016**, *6*, 160035. [CrossRef] [PubMed]
37. Bansal, A.; Schmidt, M.; Rennegarbe, M.; Haupt, C.; Liberta, F.; Stecher, S.; Puscalau-Girtu, I.; Biedermann, A.; Fändrich, M. AA amyloid fibrils from diseased tissue are structurally different from in vitro formed SAA fibrils. *Nat. Commun.* **2021**, *12*, 1013. [CrossRef]
38. Becerril, S.; Frühbeck, G. Cagrilintide plus semaglutide for obesity management. *Lancet* **2021**, *397*, 1687–1689. [CrossRef]
39. Billings, L.K.; Hsia, S.; Bays, H.; Tidemann-Miller, B.; O'Hagan, J.; Tham, L.S.; Butler, A.; Kazda, C.; Mather, K.J.; Coskun, T. Eloralintide, a selective amylin receptor agonist for the treatment of obesity: A 48-week phase 2, multicentre, double-blind, randomised, placebo-controlled trial. *Lancet* **2025**, *406*, 2631–2643. [CrossRef] [PubMed]
40. Altamirano-Bustamante, M.M.; Altamirano-Bustamante, N.F.; Larralde-Laborde, M.; Lara-Martínez, R.; Leyva-García, E.; Garrido-Magaña, E.; Rojas, G.; Jiménez-García, L.F.; Revilla-Monsalve, C.; Altamirano, P.; et al. Unpacking the aggregation-oligomerization-fibrillization process of naturally-occurring hIAPP amyloid oligomers isolated directly from sera of children with obesity or diabetes mellitus. *Sci. Rep.* **2019**, *9*, 18465. [CrossRef] [PubMed]